Paint-a-pouch: mask-based fabrication of pouch actuators for pneumatically actuated soft robots

Shuhang Zhang, Jordan Banh, Nick Gravish

***Abstract*— In this work we present a monolithic fabrication method for laminated pneumatically actuated pouch actuators. Combining the concepts of lamination, 3D printing and thermal bonding, the proposed process is capable of making low profile, pneumatic soft robots driven by pouch actuators. Two main procedures, the mask heat pressing and modified 3d printing were introduced and tested. Preferred manufacturing parameters were obtained by experiments. The fabrication, due to its simplicity and flexibility, enables fast prototyping of pneumatic actuation systems, which could potentially contribute to future soft robotic implementations.**

I. INTRODUCTION

Pouch actuators were first proposed by Niiyama, Ryuma et al. in a couple of consecutive works[1], [2], [3] around 2015. In their first paper, the group introduced a novel approach to use simple, inflatable pouches made from film materials as the actuators for folded mechanisms. Two different models, linear pouch actuators and angular pouch actuators were discovered and analysed. The actuators were fabricated by heat bonding with mechanical pressure, and then attached to folded mechanical skeletons so as to create functional robotic components powered by compressed air.

Following works include "aeroMorph"[4] and "milliMorph"[5] by Ou, Jifei et al, which used three-axis CNC machines to seal and cut the materials to make inflatable shape-changing interactive prototypes. Moghadam, Amir et al's works[6], [7] used a laser cutting technique to make thin soft pneumatic actuators rapidly.

Additionally, pouch-like actuators were integrated in complicated actuation systems. Fabricated by both heat pressure stamping and CNC machine heat sealing, the "HASEL" actuators[8], [9] introduced by Christoph Keplinger1's group could be interpreted as pouch actuators actuated with hydraulic and electrostatic principles Fatahillah, Mohammad et al. included pneumatic pouch actuation in the design of a novel soft bending actuator [10] powered by both positive and negative pressures. Novel flat fabric pneumatic artificial muscles [11] in addition to a new design space of fabric bending actuators and inflatable robots [12] are also related to pneumatic pouch actuators.

Lamination based, thin-film fabrication adapted from microelectronics industry have been proven useful in the field of soft robotics. Given the fact that pouch actuators are made by laminating of fabric or plastic films, in this work, we aim to develop a novel lamination-based fabrication method, which creates pouch actuators within soft robots.

This work was finished by authors at the School of Mechanical & Aerospace Engineering Department, University of California, San Diego. (email shuhang.zhang@epfl.ch, jordanbanh8@gmail.com, ngravish@eng.ucsd.edu).

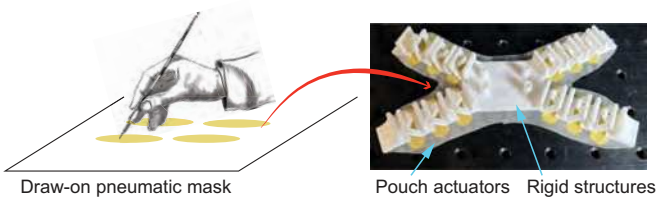

Fig. 1. In this paper we present a method for creating pneumatic circuits and pouch actuators using a draw-on masking method. Watercolor marker inhibits bonding of TPU layers and forms pneumatic channels. 3D printing rigid plastic materials on the top of the pouches allows for the combination of soft laminate based layers and pouch actuators with rigid linkages and structures.

To fabricate rotating joints under a confined size limitation, some flexible film materials are used to form semi-soft hybrid, low profile mechanisms. This is known as the fabrication concept termed Smart Composite Microstructures (SCM) [13] proposed back to 2008 by R.J. Wood et al. SCM specifically makes a integrated, planar structures with fiber reinforced rigid links and polymer flexure joints by combining laser-machining and lamination processes. Since lamination based fabrications are simple and suitable for making soft hybrid composite structures, they have also been adapted to soft robots in larger scales. Origami or folded robots, which have become an increasingly hot topic in the past years [14], [15], [16], could also be interpreted to be a direct extension of the lamination fabrications because they also use composite fabric materials in very thin profiles to achieve mechanical applications.

In 2020, a novel 3d printing approach was proposed [17] for making soft-rigid hybrid robots termed "flexoskeleton". Hybrid structures of rigidity and flexibility were created by depositing rigid 3d printing materials onto flexible polymer base sheets. This fabrication could be considered as an approximate of the SCM fabrication in a larger scale, but is relatively faster and more robust. Actuation, however, is not integrated into the fabrication process; Additional tension cables were used to drive the fabricated robot components.

In this work, a new monolithic fabrication method is proposed and tested for pneumatic pouch actuated soft mechanisms. The fabrication combines lamination with additive manufacturing techniques and could be interpreted as an extension of "flexoskeleton" [17] with inherent pouch actuator actuation. In the next section, choice of materials for lamination and 3d printing are discussed. In the third section,

the main fabrication procedures are introduced, and some characterization tests are presented to explain the choice of manufacturing parameters. In the fourth section, single pouch actuator experiments are conducted to validate the capability of the fabrication process, two robotic prototypes are demonstrated. Then, in the last section, we summarize our contribution and discuss possible future paths.

II. Choice of Material System

A suitable sheet material for making the pouch actuators should be thermoplastic to create a sealing bond, and have suitable flexibility to deform. In order to allow direct 3d printing on the pouch actuators to create support and functional structures as in "flexoskeleton"[17], the sheet material also needs to bond with at least one commonly used fused deposition modeling(FDM) filament. A thermal bonding experiment was completed to find a feasible material system for the fabrication. Three types of common FDM materials: polylactic acid(PLA), acrylonitrile butadiene styrene(ABS) and thermoplastic polyurethane(TPU) were tested with some common film and sheet materials. A soldering iron was used to heat the materials to the melting point of the filament materials to simulate a FDM 3d printing process.

TABLE I

Results from the thermal bond experiment

Filament materials	Sheet or film materials				
	PC	Nylon	PET	PE	TPU
PLA	True	False	False	False	True
ABS	True	False	False	False	True
TPU	True	False	False	False	True

Table I shows the results from the tests, a "True" result means there is a usable bond and a "False" result means there is no usable bond. Apparently, the tested 3d printing filament materials could all produce bond with TPU and PC sheet materials under the experiment condition. TPU is a class of soft, elastic material with unique properties and some different chemical formulas. The TPU film material used in this work is polyester-based and has a larger elastic modulus than the polyether-based type. Previous works [6], [18], [19]have already proven TPU's capability to form pouch actuators, therefore, we chose TPU as the sheet material for pouch actuators in this work. For 3d printing, all three types of filament materials mentioned above can be used.

III. Fabrication

A. Overview of the mask heat pressing method

Stamp heat pressing has been used to make pouch actuators in the previous work[1]. This fabrication method would require the manufacturing of metal molds for every single design, which slows down the entire fabrication process and increases the cost. Heat drawing[2] and laser welding[6] are described as rapid techniques for producing pouch actuators, however, both require specialized and expensive equipment. In this section, a different process called mask heat pressing is introduced to mitigate those shortcomings. By adding an extra layer of bond-inhibiting mask material between two

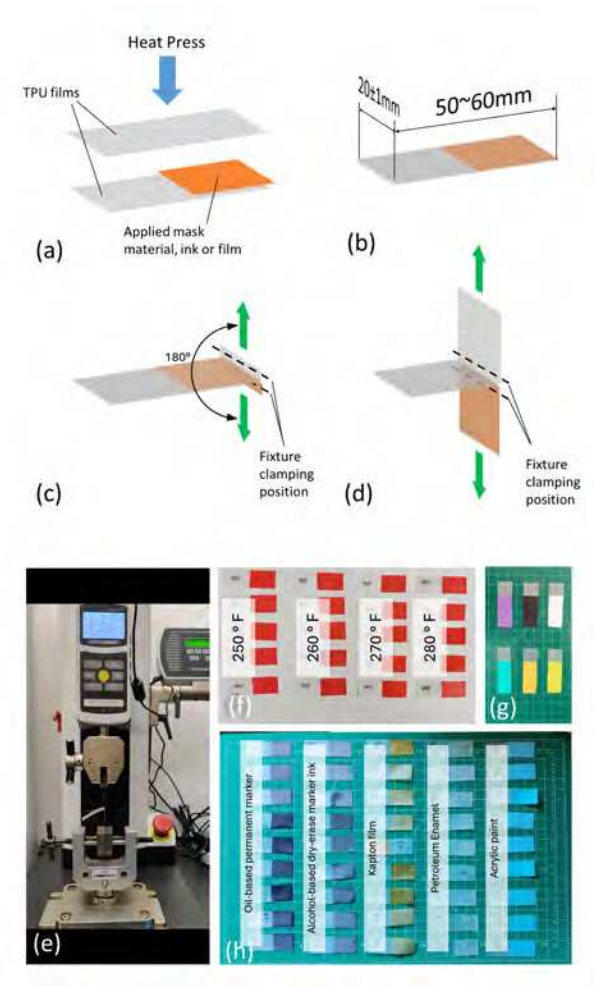

Fig. 2. (a):Preparing peel test samples by heat pressing. Each sample is divided into masked and unmasked area, heat pressed at 100N/cm^2 for 30s. (b): Dimensions of a single test sample. (c): Peel test of the masked half of a sample on the test station. The test starts from the edge and stops at the brink of the masked area. (d): Peel test of the unmasked half of the sample. The sample is reloaded on the test station and the test starts from the middle region. (e): Real time photo of a peel test, all peel tests are carried out at speed 60mm/min. (f): Test samples made with red watercolor paint as mask material at 4 different heat press temperatures. 5 repeated samples for each temperature. (g): Peel test samples made with watercolor paints of some other colors. (h): Peel test samples made with other mask materials.

TPU films(thickness 0.2mm, David Angie®) and perform a low-cost heat pressing process using a home appliance machine(ePhotoInc®), an inflatable chamber with desired shape and size could be created rapidly. The multi-layer base material is then attached to the heat bed of a 3d printer so additional functional structures can be bonded directly to the pouch actuators.

B. Mask material choice via peel tests

An ideal mask material should not bond with TPU when heat pressed, preferably some ink or paint. If there is such kind of ink, it would then possible to ink-print pneumatic chambers and channels to TPU films directly, and then heat press the films to create a complex pneumatic system.

Here, by testing of different mask materials, watercolor paint is found to be the optimal liquid mask option for pouch printing while fluorinated ethylene propylene (FEP) is the most effective film material. Watercolor paint markers (Mondo Llama^{TM}) are the primary materials used to create paint mask in this project.

A set of peel force tests are completed to evaluate the strength of the bonds created by the heat pressing process. Lower peel force indicates a better mask material. Various mask materials, particularly water color materials, are tested. Fig. 2 demonstrates details about the test method and samples. In this test, peel force results were measured at 180° angle (as depicted in Fig. 2(c)) with speed $60mm/min$.

In addition to watercolor paints, other mask material candidates are also tested. In table II, the performance of six selected mask materials are listed and compared with heat press temperature 260°F. Watercolor paint, with a relatively lower peel force of 0.015N/m, significantly outperforms other alternatives that have peel force values greater than 0.1N/m. However, FEP is an exception which does not bond after heat pressing at all at the expense of requiring additional FEP manufacturing processes such as laser/machine cutting and adhesive bonding with TPU film to form stable masked shapes on TPU films. In this project, we continue utilizing watercolor paints due to the simplicity and fluidity of the whole fabrication. Then we perform further peel tests for watercolor paint masked heat press samples to find the preferred temperature and paint type for the procedure, the results are presented in Fig. 3.

TABLE II

MASK MATERIALS PEEL STRENGTH TEST RESULTS AT 260°F.

Mask material	Peel force (N/cm)	Simplicity to use
Red watercolor paint (Control Group)	0.015	High
Acrylic paint	0.166	Medium
Petroleum Enamel	0.334	Low
Oil-based permanent marker ink	0.152	High
Alcohol-based dry-erase marker ink	0.116	High
Kapton film	0.171	Low
FEP film	0 (No bond)	Low

C. Typical 3d printing process on pouches

From the peel tests above, it is clear that with a heat press temperature about 280°F , the non-masked area of two TPU films would be bonded firmly while the masked area (with watercolor paint of any tested color as the mask material) would be still highly separable.

In this work, a common FDM 3d printer, Prusa® i3 MK3S+ is used as the fabrication center. To integrate and boost the fabrication, we modify the extruder head with a paint marker holder, which enables the user to change the 3d printer into a in-plane paint plotter. In this case, specific modifications were applied in the slicer software "PrusaSlicer" settings and G-codes to stop extrusion and heating while enabling plotting of desired shapes on the heat bed plane. With the paint marker removed, the 3d printer

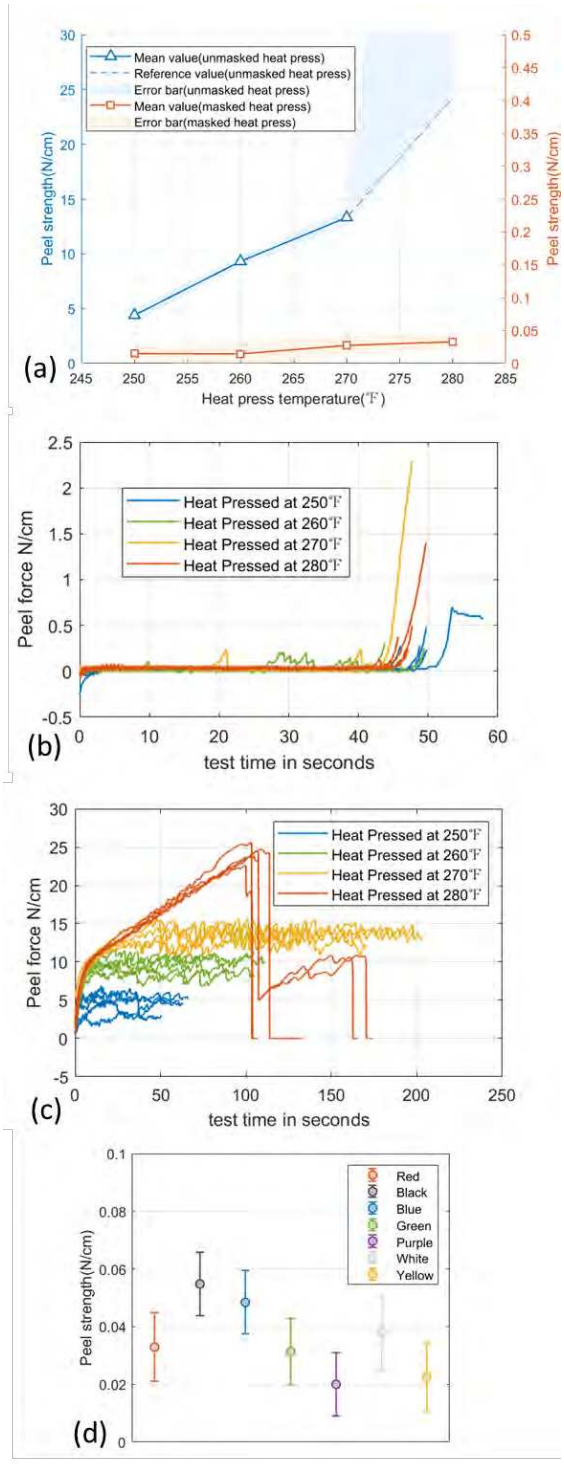

Fig. 3. (a): Peel test results of red watercolor mask samples: Average and standard deviation of peel strength value versus different heat press temperatures. No valid peel strength value obtained at 280 °F for unmasked heat press region due to the limitation imposed by TPU material, the reference value denotes break point instead of peel strength of the sample. (b): Peel test results: peel strength value versus time, masked. (c): Peel test results: peel strength value versus time, unmasked. Note that with heat press temperature 280°F, the unmasked sample broke during the test. The break point of the sample is thus considered as the reference value of the peel strength. (d) Peel test results of masked heat press at 280°F with different watercolor paint as mask material: Average and standard deviation of peel strength versus different paint colors.

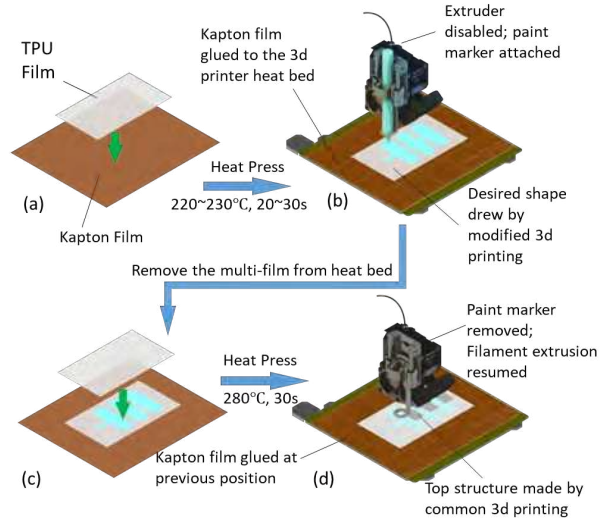

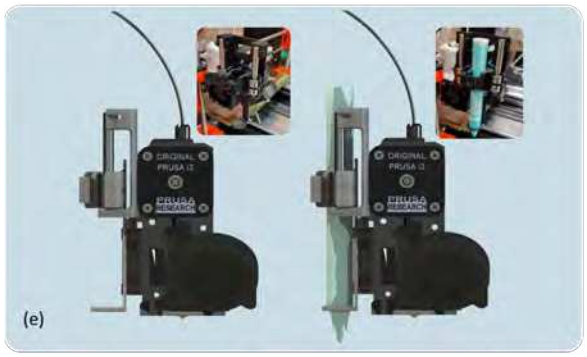

Fig. 4. The main process of the mask heat pressing fabrication. (a): Heat pressing TPU with kapton base film under mild temperature. (b): Plotting on TPU film using a paint marker attached to the 3d printer head with modified Gcode. (c): Firmly heat pressing another layer of TPU. (d): Reload the multi-layer film to the 3d printer heat bed, resume common 3d printing to create top structures, precise alignment is required. The whole structure could then be removed from the Kapton base and cut off from the multi-TPU film (e): A closer look at the modified 3d printer head, with and without the paint marker attached.

could still work smoothly like any other common 3d printer. Details of the main fabrication processes are demonstrated in schematic Fig. 4.

IV. Designing and Tests

A. Pouch geometry design

Pouch actuators were generally in rectangular shapes. The linear edges of the rectangular shape enables the pouch actuator to deform in controllable linear directions. However, when fully inflated, the cross section of two perpendicular edges would become a tip thus leading the linear edges to become distorted. To avoid this, all pouch actuators in this work were designed in slot shapes as in Fig. 5. The arcs at both ends help reduce unwanted deformation and maximize the desired output motions. The distance between the two parallel edges is called width(D) while length(L) refers to the distance from one semi-circle's center to another. All the following pouch sizes presented in this work are in the form of D×L.

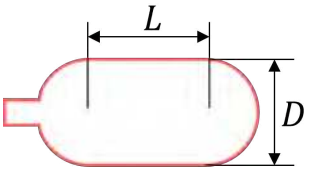

Fig. 5. Shape adapted by the pouch actuators in this work. L: length of the pouch actuator. D: width of the pouch actuator.

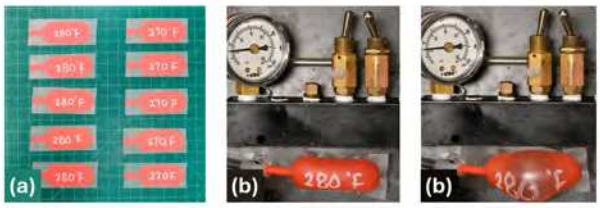

Fig. 6. (a): Single pouch samples made by the mask heat pressing method at 270° and 280°, respectively. (b): A pouch sample being tested on the pressurizing station. (c): The pouch sample fails due to excessive unwanted deformation.

B. Failure point test of single actuators

With the proposed fabrication method for pouch actuators, it is necessary to find out how much internal pressure they can hold. In this part, 10 single pouch samples sized 25mm×35mm (width × length) are made by mask heat pressing at 270°F and 280°F. Each pouch is hot glued with an air nozzle. When tested, a sample is pressurized slowly to the failure point to evaluate the strength of pouches made by the mask heat pressing method, see Fig. 6. The failure point is defined by either leakage, explosion, or excessive, irreversible deformation of the film material as shown in Fig. 6(c).

According to the test, the mean value of failure point of the pouch actuators is about 43 kPa(Heat pressed at 270°F) and 57.8 kPa(Heat pressed at 280°F), which is in accordance with the peel strength test of unmasked heat pressed TPU films above. Considering error and tolerance, we chose 50 kPa to be the pressure limit of mask heat pressed pouches with 280°F heat press temperature.

Denote a to be the shape ratio parameter of a pouch actuator, defined as:

$$a = L/D \tag{1}$$

It's pressurized area C_1a^2, total edge length as C_2a, Average peel force along the edge as T, interior air pressure as P, then:

$$PC_1D^2 = TC_2D \tag{2}$$

where C_1, C_2 are constants only related to a:

$$C_1 = a + \pi/4, \quad C_2 = \pi + 2a \tag{3}$$

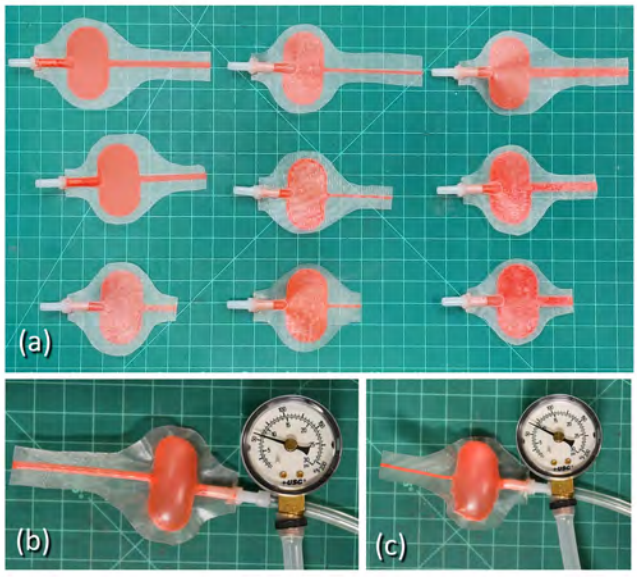

Fig. 7. (a): Narrow channel samples made by the mask heat pressing method at 280°. Each sample is composed of a pouch chamber(size 25mm×25mm) and a narrow channel. 3 different width(2mm, 4mm and 6mm) and 3 different length(20mm,40mm,60mm) of the channels were tested. (b): A sample with 4mm wide channel being tested on the pressurizing station, channel inflated successfully. (c): A sample with 2mm wide channel being tested on the pressurizing station, channel won't open within the safe pressure limit.

Given a maximum peel strength T_{max} which is decided by the material and fabrication, the maximum pressure:

$$P_{max} = \frac{C_2}{C_1}\frac{T_{max}}{D} \tag{4}$$

i.e., given a constant shape ratio a, smaller pouches could hold larger interior pressure. Therefore, the maximum allowable pressure 50 kPa only applies to pouch actuators below the size of 25mm×35mm. the pouch actuators are predicted to be weaker if the size increases.

C. Narrow channels tests

Due to the low bond strength between TPU films separated by watercolor paint, single pouches made by the mask heat pressing method could be inflated easily. However, serial pouch actuators connected with narrow channels might still suffer from the remaining bond strength between masked TPU films and won't open easily when pressurized from the air inlet. Here a set of tests are carried out to analyze how the geometry properties of narrow channels affect their ability to open, see Fig. 7 for detailed explanation and table III for the results of the tests. Note that test samples with width 2mm will not open when pressure exceeds 70 kPa pressure. Under such pressure, the pouches are very likely to fail due to excessive expansion or leaking, thus we define channels with such width unable to open.

With 4mm and 6mm channel width, only the short channels around 20mm will open within the safe pressure limit of 50 kPa ,mentioned in the previous section. With a longer length 60mm, the channels would take a pressure about 60-70 kPa to open, this might cause failure in some heat pressed pouch system. This poses a limit to the designing and actuating of the proposed printable pouch actuation system. Narrow or over complex geometries should be avoided if possible. In some cases, extra procedures such as pinching or poking might be needed to open the channels for the first time. Once already opened, the whole system would then be able to inflate and actuate without any blockage.

TABLE III
NARROW CHANNELS TEST RESULTS

channel opening pressure(kPa) / channel length(mm) / channel width(mm)	20	40	60
2	-	-	-
4	47	56	58
6	45	45	70

D. Power capability test of single actuators

To evaluate both the motion and force capabilities of the single pouch rotational joint actuators fabricated by the proposed fabrication, block force and bending angle experiments of single pouch actuators are designed and conducted. Fig. 8(a),(b) and (c) show the design and fabrication procedure of single pouch actuator samples with different sizes. Fig. 8(d) shows the test platform, which is comprised of the frame to fix the pouch actuator samples, pneumatic pressure source pump and regulator for controlling the internal pressure of the samples, a pressure sensor to read the pressure value, a load cell for sensing the block force, and an Arduino controller connected to a display for direct data reading. Two types of tests are performed. First, the angular displacement of the actuator at different internal pressure value is measured without blocking the end of the actuator. Second, the blocking force at different pressure values are measured with the load cell blocking the motion of the end of the actuator. Corresponding test results are given in Fig. 8(e) and (f). The results demonstrate that pouch width is a significant design parameter that increases angular displacement and block force output, whereas pouch length does not have distinguishable effects on performance. The output displacement could reach near 90 degrees at zero external force load, which is close to that reported in the original pouch actuator work[1]. The output moments results at zero angular displacement (derived from the output block force and pouch sizes) are also at the same level with that reported in the work[1], validating the fabrication method introduced in this work.

E. Multi-directional motion driven by prismatic pouch actuators

In this section, a system that generates multi-directional motion driven by prismatic pouch actuators will be introduced and tested. Performance will be characterized by angu-

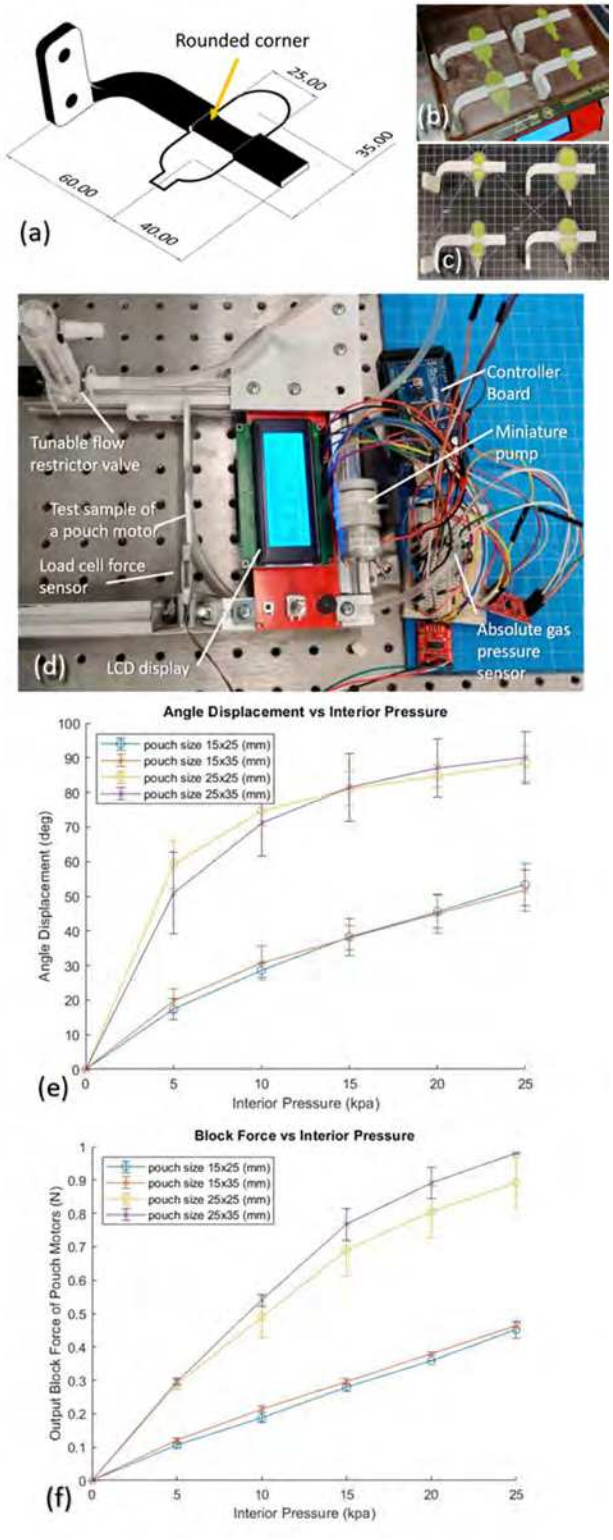

Fig. 8. (a): Design and dimensions of a single pouch actuated joint sample with size 25mm×35mm. (b): 4 samples with different dimensions fabricated by the proposed monolithic printing method. (c): Test samples with sizes 15mm×25mm, 25mm×25mm, 15mm×35mm, 25mm×35mm, respectively.(d): The test platform used for testing the block force and bending angle of each sample with respect to different interior pressure. (e),(f): Block force and deformation results versus actuating pressure of each pouch actuator size.

lar displacement and block force output. We call this system a multi-directional pouch actuator, as shown in Fig. 9.

The pouches are laid out in an orthogonal configuration to generate motion in two orthogonal directions, as shown in Figure 9. A 3D printed leg is attached to the pouches via a snap-fit hinge. The snap-fit hinge is directly printed onto the pouch using the fabrication process from the monolithic pouch fabrication process described in the previous section. The joints that are above the pouches will be treated as a rotational joint and any off-axis rotation will not be considered. The pouches will generate linear motion at the location at the connection between the rotational joint and the pouch. The appendage is also connected to the ground plane via a snap in socket. This particular connection will be treated as a ball joint. Due to clearances in the design, the leg can travel ±1 mm along the vertical axis but this has negligible effects on the output motion of the multi-directional actuator. Due to the joint constraints, the prismatic actuation of the pouches will generate an angular displacement of the appendage. The performance of the multi-directional actuator will be characterized by angular displacement and block force output experiments. Angular displacement will be measured through image processing and block force will be measured using a load cell. For each multi-directional pouch, the angular displacement and block force are measured three times for each increment of pressure. Then we calculate the average and standard deviation for the measurements for the three different multi-directional pouches. The results are shown in Fig. 10

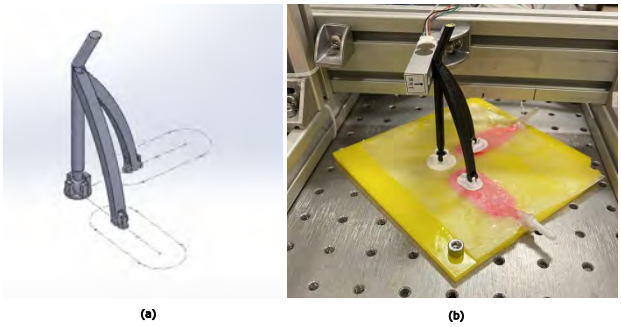

Fig. 9. a) The multi-directional pouch actuator design is shown. The z-axis is defined as the line orthogonal to both pouch axes (along the length of the pouch). b) The experimental set up is shown. A load cell is placed perpendicular to the expected direction of motion to measure block force.

F. Quadruped crawling robot demonstration

To demonstrate the practical value of the proposed fabrication, a crawling quadruped robot, whose configuration is adapted from the classic multi-gait soft robot design[20] was designed and tested. Fig. 11 shows the design and test details of the quadruped robot.

By 3d printing rigid materials(ABS in this case) on top of the heat pressed layers, strain limiting structures were created so that the limbs would bend toward the opposite direction. By creating joint-limiting jamming structures (shown in Fig. 11(b)) over the base of the robot, the bending degree of

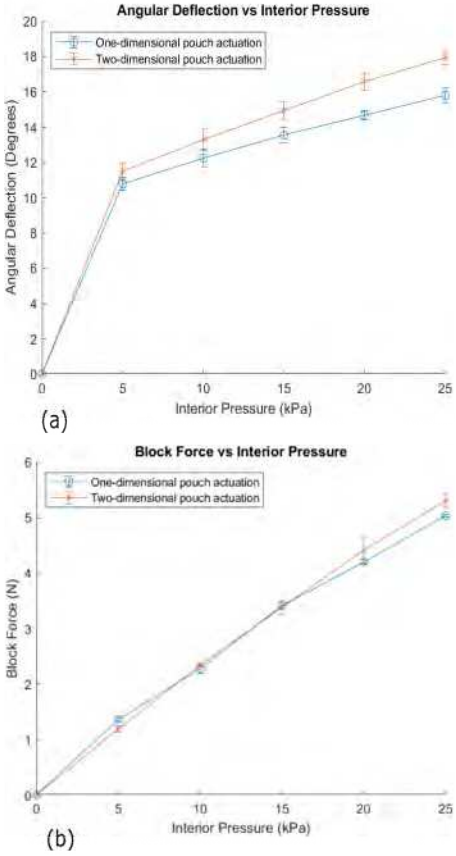

Fig. 10. a) Angular Deflection test results for one-dimensional pouch actuation and two-dimensional pouch actuation b) Block force test results for one-dimensional pouch actuation and two-dimensional pouch actuation

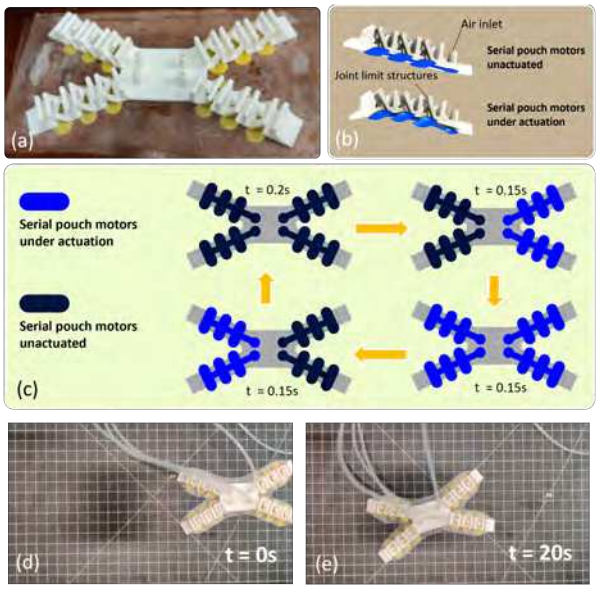

Fig. 11. (a): The quadruped robot that had just been made by the monolithic fabrication method on the modified 3d printer. Planar size 155mm×85mm. (b): Schematic of a single limb in idle and under actuation. The 3d-printed rigid structures act as joint limits which confine the deformation to desired direction and degree. (c): The actuation sequence of 4 individual limbs by a miniature pump and valves system. The block pressure of the pump is around 40 kPa, which is considered as the reference pressure of the actuation. (d),(e): The quadruped robot being tested on a plastic mat, movement speed reached 6.5mm/s with actuation cycle time 0.65s.

limbs are controlled to desired values. Air inlet nozzles are also created by directly 3d printing on the heat pressed TPU layers, with holes cut on corresponding positions of the top TPU layer before heat pressing.

V. Conclusion

In this work, a novel 3d-printing-based fabrication method of pneumatic pouch actuators is proposed and tested. Combining the concepts of laminating, additive manufacturing and masked heat bonding, the proposed fabrication method enables fast prototyping of pouch actuators and robotic components in a integrated fabrication center. Table IV compares our method against some typical fabrication methods from literature.

Among the various sheet and film materials, TPU was found to be an excellent choice for pouch fabrication due to its thermal-bonding property with common FDM 3d printing filament materials such as PLA and ABS. Watercolor paint was found to be a suitable printable mask material for the mask heat pressing procedure.

The mask heat pressing method uses a mask between heat pressed TPU films to create inflatable chambers. Once the base layer with pouch actuators is ready from heat pressing, it is then attached to the heat bed of a 3d printer and goes through the final 3d printing process. With suitable choice of filament material and setting of parameters, a solid, strong bond will be created between the multi-layer base and the 3d printed structures. The 3d printing process would endow the structure with needed strength, rigidity and special geometry patterns at desired location. Positioning and alignment is crucial in this process.

Through the characterization tests, the capability and limitation of the proposed fabrication method has been studied and discussed. Designing and testing of the robotic prototypes validated the potential value of the fabrication in soft robot applications.

VI. Conceptual Extension

A. Improved mask heat pressing process

There may be mask materials with more effective material properties for this application. Ideally, some paint or ink material with excellent non-stick properties will be discovered in the future. This would enable more complex designs of printable pneumatic systems.

On the other hand, the printable mask layer in this work is made through a plotting process, which is relatively slow compared to commercial printing techniques. Common inkjet or laser printer can possibly be modified to print the non-heat sealing mask patterns in this work and further accelerate the fabrication process. Also, in this work, plotting/3d printing and heat pressing are executed on different devices, which can cause inconsistency and alignment issues during the

TABLE IV

COMPARISON BETWEEN POUCH ACTUATOR FABRICATION METHODS

Methods	Speed	Equipment	Supporting robotic structures
This work	Fast	3d printer and low end heat press	Created with the same machine for making pouch actuators
Stamp pressing	Making stamps costs time	CNC manufacture	Needs extra equipment and bonding
Thermal drawing	Fast	Special drawing machine	Needs extra equipment and bonding
laser welding	Very fast	Expensive laser machine	Needs extra equipment and bonding

fabrication. An integrated fabrication machine capable of plotting, 3d printing and heat pressing could be developed in the future.

B. Embedded Sensors and circuits

This work has focused primarily on actuators. Embedded sensors and electronics, however, are components that can potentially be integrated into this monolithic, lamination based fabrication process of low profile soft robot. Research could be carried out to integrate printable sensors and circuits into the multi-layer heat pressed structure. The embedded circuits could be either traditional conductive circuits or microfluidic systems.

C. Entirely printable soft robots

This project could potentially contribute to some highly integrated manufacturing center in the future. The film materials will be processed, masked and heat pressed automatically and create a multi-functional composite structure with all needed sensing, actuation and energy components. This would allow massive production of small, low-cost soft robots.

ACKNOWLEDGMENT

Funding support was provided through the Mechanical and Aerospace Engineering Department at UCSD. This material is based upon work supported by the National Science Foundation under Grant No. 1935324 and the Office of Naval Research under grant number N00014-20-1-2373. Any opinions, findings, and conclusions or recommendations expressed in this material are those of the author(s) and do not necessarily reflect the views of the National Science Foundation.

REFERENCES

[1] Ryuma Niiyama, Daniela Rus, and Sangbae Kim. Pouch motors: Printable/inflatable soft actuators for robotics. *2014 IEEE International Conference on Robotics and Automation (ICRA)*, 2014.

[2] Ryuma Niiyama, Xu Sun, Cynthia Sung, Byoungkwon An, Daniela Rus, and Sangbae Kim. Pouch motors: Printable soft actuators integrated with computational design. *Soft Robotics*, 2(2):59–70, 2015.

[3] Xu Sun, Samuel M. Felton, Ryuma Niiyama, Robert J. Wood, and Sangbae Kim. Self-folding and self-actuating robots: A pneumatic approach. *2015 IEEE International Conference on Robotics and Automation (ICRA)*, 2015.

[4] Jifei Ou, Mélina Skouras, Nikolaos Vlavianos, Felix Heibeck, Chin-Yi Cheng, Jannik Peters, and Hiroshi Ishii. Aeromorph - heat-sealing inflatable shape-change materials for interaction design. In *Proceedings of the 29th Annual Symposium on User Interface Software and Technology*, UIST '16, page 121–132, New York, NY, USA, 2016. Association for Computing Machinery.

[5] Qiuyu Lu, Jifei Ou, João Wilbert, André Haben, Haipeng Mi, and Hiroshi Ishii. millimorph – fluid-driven thin film shape-change materials for interaction design. *Proceedings of the 32nd Annual ACM Symposium on User Interface Software and Technology*, 2019.

[6] Amir Ali Amiri Moghadam, Seyedhamidreza Alaie, Suborna Deb Nath, Mahdie Aghasizade Shaarbaf, James K. Min, Simon Dunham, and Bobak Mosadegh. Laser cutting as a rapid method for fabricating thin soft pneumatic actuators and robots. *Soft Robotics*, 5(4):443–451, 2018.

[7] Amir Ali Amiri Moghadam, Alexandre Caprio, Seyedhamidreza Alaie, James K. Min, Simon Dunham, and Bobak Mosadegh. Rapid Manufacturing of Thin Soft Pneumatic Actuators and Robots. *Journal of Visualized Experiments*, (153):60595, November 2019.

[8] Nicholas Kellaris, Vidyacharan Gopaluni Venkata, Garrett M. Smith, Shane K. Mitchell, and Christoph Keplinger. Peano-hasel actuators: Muscle-mimetic, electrohydraulic transducers that linearly contract on activation. *Science Robotics*, 3(14), 2018.

[9] Shane K. Mitchell, Xingrui Wang, Eric Acome, Trent Martin, Khoi Ly, Nicholas Kellaris, Vidyacharan Gopaluni Venkata, and Christoph Keplinger. An easy-to-implement toolkit to create versatile and high-performance hasel actuators for untethered soft robots. *Advanced Science*, page 1900178, 2019.

[10] Mohammad Fatahillah, Namsoo Oh, and Hugo Rodrigue. A novel soft bending actuator using combined positive and negative pressures. *Frontiers in Bioengineering and Biotechnology*, 8, 2020.

[11] Woojong Kim, Hyunkyu Park, and Jung Kim. Compact flat fabric pneumatic artificial muscle (ffpam) for soft wearable robotic devices. *IEEE Robotics and Automation Letters*, 6(2):2603–2610, 2021.

[12] Haneol Lee, Namsoo Oh, and Hugo Rodrigue. Expanding pouch motor patterns for programmable soft bending actuation: Enabling soft robotic system adaptations. *IEEE Robotics & Automation Magazine*, 27(4):65–74, 2020.

[13] R. J. Wood, S. Avadhanula, R. Sahai, E. Steltz, and R. S. Fearing. Microrobot design using fiber reinforced composites. *Journal of Mechanical Design*, 130(5), 2008.

[14] Cynthia Sung and Daniela Rus. Foldable joints for foldable robots. *Experimental Robotics Springer Tracts in Advanced Robotics*, page 421–433, 2015.

[15] Duncan Haldane, Carlos Casarez, Jaakko Karras, Jessica Lee, Chen Li, Andrew Pullin, Ethan Schaler, Dongwon Yun, Hiroki Ota, Ali Javey, and Ronald Fearing. Integrated manufacture of exoskeletons and sensing structures for folded millirobots. *Journal of Mechanisms and Robotics*, 7(2), 2015.

[16] Cagdas D. Onal, Michael T. Tolley, Robert J. Wood, and Daniela Rus. Origami-inspired printed robots. *IEEE/ASME Transactions on Mechatronics*, 20(5):2214–2221, 2015.

[17] Mingsong Jiang, Ziyi Zhou, and Nicholas Gravish. Flexoskeleton printing enables versatile fabrication of hybrid soft and rigid robots. *Soft Robotics*, 7(6):770–778, 2020.

[18] Hareesh Godaba, Aqeel Sajad, Navin Patel, Kaspar Althoefer, and Ketao Zhang. A two-fingered robot gripper with variable stiffness flexure hinges based on shape morphing. *2020 IEEE/RSJ International Conference on Intelligent Robots and Systems (IROS)*, 2020.

[19] Pham Huy Nguyen and Wenlong Zhang. Design and Computational Modeling of Fabric Soft Pneumatic Actuators for Wearable Assistive Devices. *Scientific Reports*, 10(1):9638, June 2020.

[20] Robert Shepherd, Filip Ilievski, Wonjae Choi, Stephen Morin, Adam Stokes, Aaron Mazzeo, Xin Chen, Michael Wang, and George Whitesides. Multigait soft robot. *Proceedings of the National Academy of Sciences of the United States of America*, 108:20400–3, 11 2011.